Fracture Mechanics of Concrete Structures, de Borst et al (eds) © 2001 Swets & Zeitlinger, Lisse, ISBN 90 2651 825 0

Simulations on Crack Distribution in FRP-Strengthened Concrete Beams with Interfacial Fictious Crack Model

Jun Yin & Zhishen Wu
Department of Urban and Civil Engineering, Ibaraki University, Hitachi, Japan

ABSTRACT: Cracking behavior significantly affects the failure mode and strengthening performance of FRP sheets in FRP-strengthened concrete beams. The objective of this paper is to make an understanding on how the properties of concrete and bond interface influence the cracking behaviors through finite element simulations. Four material properties, concrete fracture energy, bond strength, interfacial fracture energy and stiffness of bond interface, are chosen as important parameters that are discussed in detail. Debonding behavior of FRP-concrete bond interface is described by interfacial fictious crack model. Cracks in concrete are modeled by smeared crack model. It can be concluded that a certain behaviors of FRP-concrete interfacial bond is a pre-required condition of FRP reinforcement and essentially determines whether premature debonding failure happens within the bond layer before the realization of strengthening performance. Concrete fracture energy has a significant effect on the status of crack distribution in concrete. Increasing concrete fracture energy could enhance the strengthening performance of FRP reinforcement.

1 INTRODUCTION

The application of fiber reinforced polymer (FRP) sheets, as an externally bonded reinforcement, is generally accepted as an effective technique of strengthening and upgrading structurally inadequate or damaged concrete structures. FRP sheets offer unique advantages, such as high strength-to-weight ratio and considerably good resistance to corrosion, over the conventional steel bars and plates that cannot provide satisfactory service life.

In the past decade, FRP sheets have been widely applied to the strengthening and repairing of concrete structures in service, such as buildings, bridges and tunnel linings. The FRP strengthening has been demonstrated remarkably efficient in practice. However, the mechanical behavior of reinforced concrete structures, especially the FRP-concrete interfacial bond behavior, is still on the way of research. In recent years, much work has been done through theoretical analysis, as well as the experimental approaches.

For a simple shearing case, the maximum load carring capacity of a FRP-strengthened concrete prism was theoretically derived by Taljsten (1996). It could be written as a function of interfacial fracture energy, Young's modulus and thickness of FRP composites. More investigations of the stress transfer in FRP-concrete bond interface were done by Nishida et al. (1999), Wu et al. (in submittal) and Yuan et al. (in press), in which several types of local shear stress versus relative displacement relations were proposed and the corresponding shear stress distributions along the bond interface during debonding propagation were predicted. A methodology was developed by Wu & Niu (2000) to evaluate the debonding failure load and the interaction between flexural concrete crack and interfacial shear stress of RC beams based on linear elastic beam theory. In the experimental aspects, a single-lap shear test was carried out to study on the bond strength and force transfer of FRP-concrete bond interface (Chajes et al. 1996). The similar experiments were done to identify the interfacial mode II fracture energy and the local shear stress versus relative displacement relationship was predicted indirectly from the FRP strain distribution along the bond interface (Yoshizawa et al. 2000). A series of tests of FRP-strengthened concrete beams were performed (Wu et al. 1998) to study the more complicated fracturing behaviors. The failure modes of both interfacial debonding and FRP sheets rupture with different cracking behaviors in concrete were observed.

In this paper, fracturing behavior in FRP-strengthened concrete beam is further studied through finite element simulations. Referred to the experimental data (Yoshizawa et al. 2000) and finite element analysis of interfacial crack propagation (Yin & Wu 1999, Yin et al in press, Wu & Yin in submittal), a bilinear ascending-softening τ–δ rela-

tionship is used. By changing the properties of FRP-concrete bond interface and concrete, an intensive parametric study is carried to analyze how these properties take effect on the load carrying capacity, deformation and cracking behavior of FRP-strengthened beams.

2 EXPERIMENTAL REVIEW

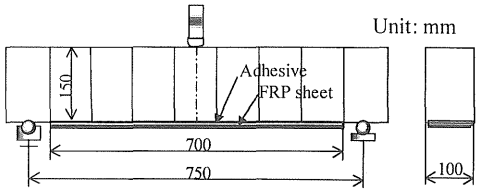

Figure 1. Specimen dimension and test arrangement

As described in the tests of FRP-strengthened concrete beams under 3-point bending load (Wu et al. 1998), FRP sheets were externally bonded on the tension surface through epoxy adhesive. The dimension and loading conditions of tested beams are described in Figure 1.

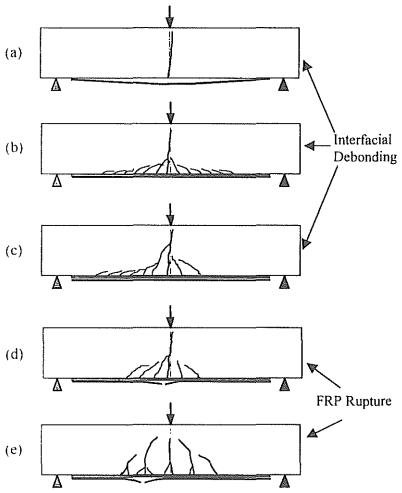

Figure 2. Crack patterns of different failure modes

From the experimental observation, there are two typical failure modes, the interfacial debonding of FRP sheets from the bond interface and the rupture of FRP sheets. In the tested beams that failed in interfacial debonding, there are three types of debonding forms. The first type happens in adhesive layer due to ill-bonded condition and initiates from the root of mid span. The second one takes place in concrete with formation of micro-cracks along the bond interface. It also starts to propagate from mid span. The corresponding cracking patterns of concrete are presented in Figure 2a and Figure 2b, respectively. A common point of these two types of debonding failures is that only one dominant flexural crack locally occurs and develops at mid span. The third form of debonding initiates from the root of a diagonal crack that has formed near the first flexural crack at mid span. Then, it follows micro-crack development along the bond interface, as shown in Figure 2c.

On the other hand, for the beams of FRP rupture failure, there are also two representative cracking behaviors. One dominant flexural crack at mid-span with multiple diagonal micro-cracks near the bond interface as shown in Figure 2d, and multiple flexural cracks are distributed along the bond interface, as shown in Figure 2e. The load capacity of the beams that failure in FRP rupture is universally higher than that of beams in debonding failure.

3 FRACTURE MODELS

In the tested concrete beams, there exist three types of fracturing behaviors, 1) FRP sheet rupture 2) cracks in concrete and 3) debonding along bond interface. To simulate these fracturing behaviors, the corresponding fracture models are introduced.

The mechanical property of the FRP sheet is relatively simple. Different from the conventional reinforced steel bars, FRP sheet does not yield and is assumed to be elastic until rupture where the tensile strength is exceeded. And it can not carry any compression. Therefore, the stress-strain can be expressed as,

$$\sigma_{FRP} = \begin{cases} E_{FRP}\,\varepsilon_{FRP} & (0 \le \varepsilon_{FRP} \le f_{frp} / E_{FRP}) \\ 0 & (\varepsilon_{FRP} < 0) \end{cases} \quad (1)$$

in which f_{FRP}, E_{FRP}, σ_{FRP} and ε_{FRP} are tensile strength, elastic modulus, tensile stress and tensile strain of FRP sheets, respectively.

Crack in concrete is assumed as mode I fracture. Smeared crack model is used to simulate the crack propagation in concrete matrix, in which a linear softening relation of concrete stress and strain after crack is adopted.

Interfacial debonding is an important fracturing behavior in FRP-strengthened concrete members. It resembles the bond-slip in steel bar reinforced concrete. But it also differs from bond-slip since reinforcement of FRP sheets are achieved by the stress transfer, but not by mechanical friction due to bond-

slip. Herein, the debonding is modeled as a mode II cohesive crack. The mechanical behavior can be described as a relationship of local shear stress, τ, versus the relative shear displacement, δ_l, between FRP sheets and concrete. A bilinear ascending-softening τ-δ_l relationship is adopted, as presented in Figure 3.

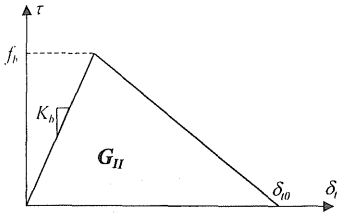

Figure 3. τ-δ_l relationship for bond interface

This τ-δ_l curve could be uniquely determined by bond strength, f_b, initial bond stiffness, K_b, and interfacial fracture energy G_{II}. The interfacial fracture energy, G_{II}, is defined as the energy required to generate complete debonding per unit bond area. The area below τ-δ_l curve denotes the value of G_{II}. In general cases, G_{II} should be calculated by integrating shear stress τ over displacement δ_{l0}. But for the bilinear τ-δ_l relationship used in see Figure 3, G_{II} can be obtained as

$$G_{II} = \frac{1}{2} f_b \cdot \delta_{l0} \tag{2}$$

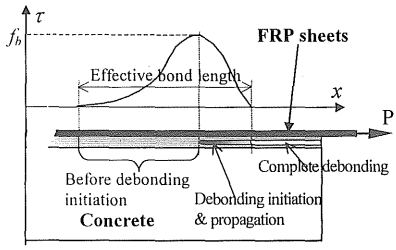

Figure 4. Debonding propagation along bond interface

Figure 4 schematically shows the interfacial debonding process. Before the shear stress exceeds the bond strength f_b, the distribution of shear stress along the bond interface gradually increases from the far end. Then, shear stress starts to decrease, where debonding is initiated. With increase of relative displacement between FRP sheets and concrete, the shear stress finally drops to zero and the complete debonding is formed.

4 NUMERICAL SIMULATION AND DISCUSSION

Considering the symmetry of load condition and structure dimension, half of the FRP-strengthened beam is chosen with proper boundary conditions, as shown in Figure 5.

The FRP-strengthened concrete beam is discretized by three types of finite elements: 4-node plane stress element for concrete matrix, line-to-line interface element (DIANA 1998) for FRP-concrete bond interface and truss element for FRP sheets.

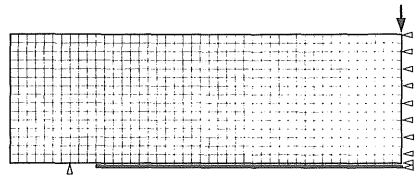

Figure 5. Mesh discritaztion and boundary condition

Some material properties used in finite element simulations are chosen as follows. For concrete, Young's modulus is $E_c = 2.5 \times 10^4$ MPa, Poisson ratio is $\nu = 0.15$, tensile strength is $f_t = 3.31$ MPa, which are obtained from the test data. The mode I fracture energy of concrete, G_f, is thought as an unknown material property. For FRP sheets, Young's modulus is $E_{FRP} = 2.3 \times 10^5$ MPa, tensile strength at rupture $\sigma_r = 3.35 \times 10^3$ MPa, thickness is 0.11 mm, all of which are according to the manufacturer-provided specifications. For the FRP-concrete bond interface, few experimental data are available. Also, the bond interface properties, such as interfacial fracture energy G_{II}, bond strength f_b and initial stiffness K_b, greatly depend on the FRP-concrete bond conditions influenced by bonding techniques, for example, the surface processing and use of different adhesive, and the environmental temperature. Therefore, these three properties, plus with the fracture energy of concrete G_f, are considered as variable parameters.

A case analysis on how these four properties take effect on the FPR-strengthened beam's load carrying capacity, deformation and fracturing behaviors is carried out and intensively discussed in the following sub sections.

4.1 *Effect of interfacial fracture energy* G_{II}

As studied in the previous works of FRP bonded concrete prism under simple shear load (Taljsten, 1996, Wu et al in submittal, Yuan et al in press), the interfacial fracture energy G_{II} is an important parameter to describe the stress transfer capacity of FRP-concrete bond interface. It determines the load

carrying capacity of the bond, if Young's modulus and thickness of FRP sheet are kept unchanged. How this parameter affects the mechanical behavior in FRP-strengthened concrete beams is discussed in the following cases.

With the same concrete fracture energy G_I = 0.25 N/mm, bond strength f_b = 1.0 MPa and initial bond stiffness K_b = 160 N/mm^3, in which the value of initial bond stiffness K_b is referred to the experimental results by Yoshizawa et al. (2000), the interfacial fracture energy is varied with G_{II} = 0.5, 1.2 and 2.0 N/mm. The simulation results of load-displacement curves and crack patterns are compared in Figure 6 and Figure 7, respectively.

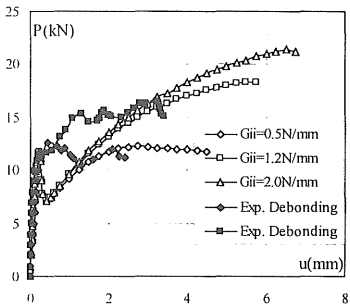

Figure 6. Load-displacement curves with different G_{II}

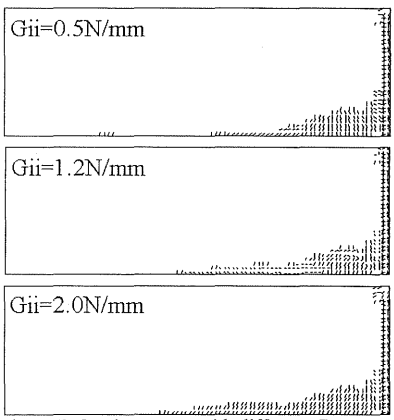

Figure 7. Crack patterns with different G_{II}

All three beams are subjected to interfacial debonding. As shown in Figure 7, there are no other flexural cracks in concrete except the one at mid span because the bond strength f_b = 1.0 N/mm^2 is rather low. But with increase of interfacial fracture energy G_{II}, the load carrying capacity is enhanced and it finally approaches to constant values in each case. Two tested beams in debonding failure that happens in adhesive layer show the similar results.

Therefore, it is considered that there should be a relationship between the ultimate load carrying capacity of FRP-strengthened concrete beam and the interfacial fracture energy G_{II} if interfacial debonding happens.

4.2 *Interfacial Bond Strength f_b*

Interfacial bond strength is defined as the maximum shear stress that the FRP-concrete bond interface can bear. When the shear stress exceeds the bond strength, the interfacial debonding is initiated and local shear stress starts to decrease. In experiment, the debonding failure was observed both in adhesive layer and in concrete near the bond interface. Herein, the bond strength is assumed as the property of adhesive. The debonding that happens in concrete should be related to the material properties of concrete, such as fracture energy. This discussion will be made in later sub-section.

Four cases with bond strength f_b = 1.0, 1.8, 2.5 and 3.0 MPa, are simulated. Other material properties are chosen as, Concrete fracture energy G_I = 0.25 N/mm, interfacial fracture energy G_{II} = 1.2 N/mm and stiffness of bond interface K_b = 160 N/mm^3.

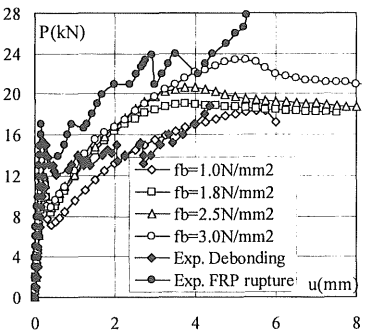

Figure 8. Load-displacement curve with different f_b

As shown in Figure 8, the peak load increases with the increasing bond strength. Noticing the τ–δ_l relationship used to model the interfacial debonding, before shear stress in FRP-concrete interface exceeds the bond strength, the higher the shear stress can reach, the more stress can be transferred from FRP sheets to concrete so as to cause more concrete to crack. Since the external load need to do more works to create the cracks, the peak load increases.

Afterwards, the load decreases and approaches to a constant value. The ultimate loads of cases f_b = 1.0, 1.8, 2.5 MPa are very close because the interfacial fracture energies are chosen the same value and in-

terfacial debonding mainly happens in the bond layer. The ultimate load of case f_b = 3.0 MPa is higher than the previous three cases. This may be due to much more cracks in concrete caused by stress transfer. Also, interfacial debonding partly occurs in concrete near the bond interface, as seen in Figure 9. Hence, the extra works done to create more cracks in concrete keeps the ultimate load higher. It is, to some extent, related to the concrete properties such as concrete strength and fracture energy.

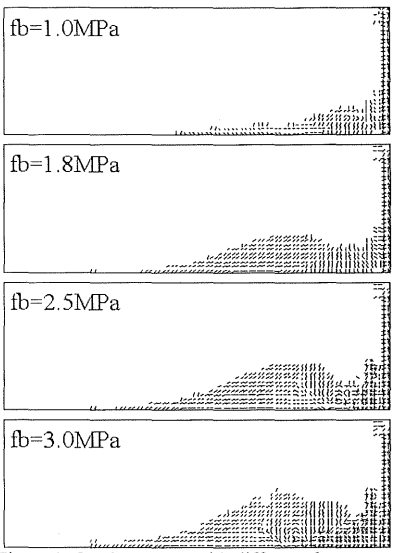

Figure 9. Crack patterns with different f_b

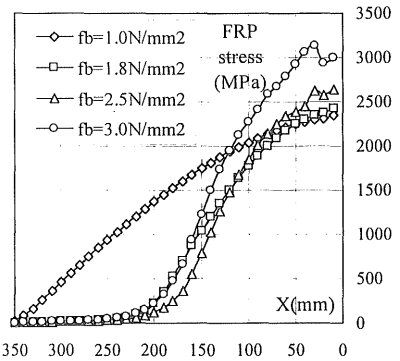

Figure 10. Stress distribution of FRP sheets

From the comparison of FRP sheets stress distributions in Figure 10, the maximum stress of case f_b = 3.0 MPa is about 3200 MPa, apparently higher than that of other cases, and is near to the rupture stress of FRP sheets.

Compared to the experiments in Figure 8, it is found that the beam of high bond strength with f_b = 3.0 MPa is similar to the tested beam of FRP rupture, while the one of low bond strength with f_b =1.0 MPa is close to the tested beam in interfacial debonding failure.

It is suggested that the bond strength affects the peak load of FRP-strengthened concrete beams. The ultimate load capacity mainly depends on the interfacial fracture energy G_{II} if interfacial debonding happens.

4.3 *Concrete Fracture Energy* G_I

Fracture energy is considered as a key material property of concrete to describe the brittleness of concrete in crack propagation. Cracks that happen in concrete beam include both the flexural cracks caused by bending and the crack along the bond interface. It significantly influences the structural response of FRP-strengthened concrete beams.

The effect of concrete fracture energy, with G_I = 0.1, 0.25, 0.35 and 1.0 N/mm, is discussed under two types of situations: (1) weak interfacial bond with f_b = 1.0 MPa and G_{II} = 1.2 N/mm, and (2) good interfacial bond with f_b = 2.5 MPa, G_{II} = 2.0 N/mm. For both situations, the initial stiffness of bond interface is K_b = 160N/mm^3.

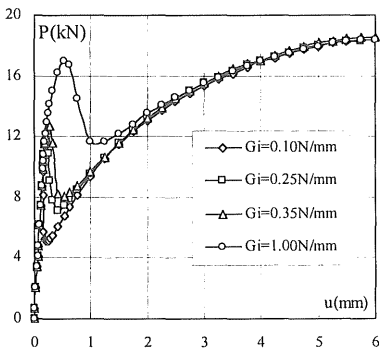

Figure 11. Load-displacement curve for situation (1)

For situation (1), concrete fracture energy only affects the crack propagation at mid span. Because the interfacial bond is very weak, when interfacial crack is initiated from the root of mid span, it propagates rapidly and leads to final debonding failure. Hence, simply increasing concrete fracture energy does not improve FRP strengthening effect if FRP-concrete interface is originally weak, in Figure 11.

For situation (2), both bond strength f_b and interfacial fracture energy G_{II} are increased. From the crack pattern of G_I = 0.1 N/mm, as shown in Figure 12, a diagonal concrete crack occurs near the flexural

crack at mid span. Finally, debonding failure happens and propagates from the root of the diagonal crack. When G_I is increased to 0.25 N/mm, a second flexural crack occurs at 130 mm away from the first one at mid span. In the load-displacement curve, there is a second unloading at displacement 3.5mm, reflecting the local stress release due to localized crack propagation of the second flexural crack. The load level is also enhanced. The maximum stress of FRP sheets reaches the rupture stress, σ_r =3.35×10^3 MPa, marking the FRP sheets rupture as shown in Figure 13. With further increase of G_I = 0.35 and 1.0 N/mm, no apparent localized flexural cracks are observed from crack patterns. Cracks tend to be distributed along the bond interface. And ultimate failure also becomes the FRP rupture, noticing the maximum stress in FRP sheets exceeds the rupture stress.

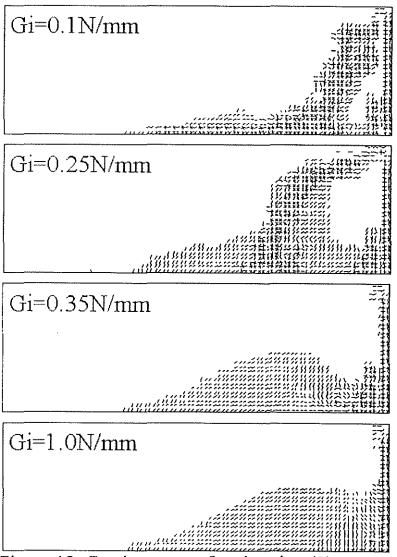

Figure 12. Crack patterns for situation (2)

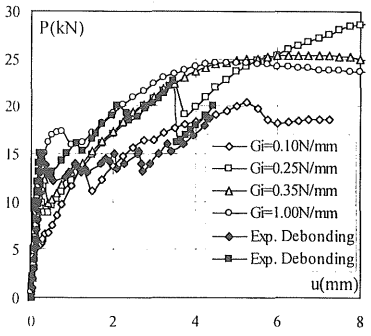

Figure 13. Load-displacement curves for situation (2)

It can be concluded that if good interfacial bond is guaranteed, increasing concrete fracture energy may result in different failure modes, from interfacial debonding to FRP rupture, and affect the cracking behavior in concrete. FRP strengthening effect is highly improved. The interfacial fracture energy is no longer the only factor to determine the load carrying capacity when cracks in concrete become distributed.

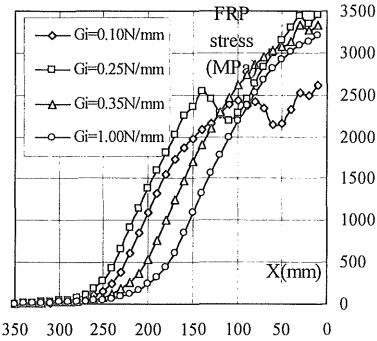

Figure 14. FRP stress distributions for situation (2)

4.4 *Initial Stiffness of Bond Interface K_b*

Stiffness of bond interface used in present FE simulation is considered as an average property of concrete and adhesive. With different bond conditions and concrete Young's modulus, the value of K_b may be changed. In this sub-section, the simulation results of four bond stiffness, with K_b = 320, 160, 80 and 40 N/mm^3, are compared. The constant material properties are f_b = 2.5 MPa, G_{II} = 1.2 N/mm and G_I = 0.1 N/mm.

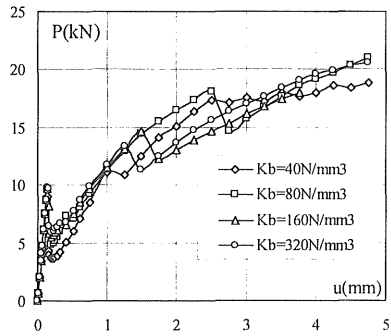

Figure 15 Load-displacement curves with different K_b

From Figure 15 of load-displacement curves, the bond stiffness does not affect much on load carrying

capacity. But the cracking behavior in concrete is relatively much influenced, as shown in Figure 16. The higher bond stiffness provides quicker increase of shear stress in the bond interface. The quick stress transfer from FRP sheets to concrete makes the concrete stress level increase near mid span earlier. That is why the diagonal crack occurs near the first flexural crack in higher bond stiffness K_b = 320 and 160 N/mm^3. In case of K_b = 80 N/mm^3, the secondary flexural crack happens away from the first one. If bond stiffness is too small, with K_b = 40 N/mm^3, the stress transfer can not be well achieved. Therefore, cracks in concrete do not continuously propagate upward after initiation, and interfacial debonding failure occurs ultimately.

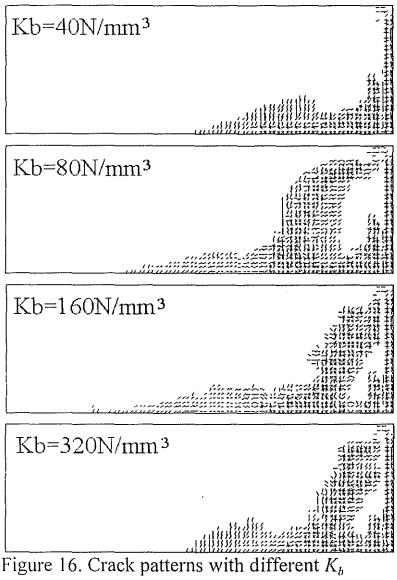

Figure 16. Crack patterns with different K_b

5 CONCLUSIONS

A comprehensive FE study on the cracking behavior of FRP-strengthened concrete beams is performed. Through the parametric numerical simulations, the following conclusions could be obtained:

(1) The ultimate load carrying capacity is quantitatively related to interfacial fracture energy G_{II} if concrete cracks are localized with ultimate debonding failure. Small G_{II} would lead to easy interfacial debonding propagation. But for the case that distributed cracks occur, the load carrying capacity would be also affected by concrete fracture energy G_I.

(2) Bond strength, in a certain scope, affects the peak load. But the propagation of debonding is also related to the interfacial fracture energy and concrete fracture energy.

(3) Under good interfacial bond, the increase of concrete fracture energy G_I results in distributed crack in concrete, thus improving FRP strengthening performance.

(4) Stiffness of bond interface does not affect much of load carrying capacity, but has an influence on the cracking behaviors in concrete.

In summary, the reinforcement of FRP sheets can be well performed by ensuring the FRP-concrete interfacial bond. In this paper, interfacial fracture energy, bond strength and initial bond stiffness are chosen to describe the bond properties. It is also found that increasing concrete fracture energy can further enhance the FRP strengthening effect. This finding is helpful to the design of future concrete structures.

Further works are needed to describe interactions among the discussed properties in this paper so as to propose more practical model to deal with the interfacial fracturing in FRP-strengthened concrete structures.

6 REFERENCES

Chajes, M.J., Finch, Jr. W.W., Januszka, T. & Thomson, Jr. T. 1996. Bond and force transfer of composite material plates bonded to concrete, *ACI Structural Journal*. Vol.93, No.2, pp.208-217.

DIANA-7 User's Manual, 1998. Lakerveld b.v., The Hague.

Nishida, H., Kamiharako, A., Shimomura, T. & Maruyama, K. 1999. Bond mechanism between continuous fiber and concrete, *Proceedings of JCI*, Vol.21, No.3, pp.1507-1512. (in Japanese).

Taljsten, B. 1996. Strengthening of concrete prisms using the plate-debonding technique, *Int. Journal of Fracture*, Vol.81, pp.253-266.

Wu, Z.S, Matsuzaki, T. & Tanabe, K. 1998. Experimental Study of Fracture Mechanism of FRP-Strengthened Concrete Beams, *JCI Symposium on FRP Reinforced Concrete Structures, JCI*, pp.119-126. (in Japanese).

Wu, Z.S. & Niu, H.D. 2000. Study on debonding failure load of RC beams strengthened with FRP sheets, *Journal of Structural Engineering* Vol.46A, pp.1431-1441.

Wu, Z.S. & Niu, H.D. 2000. Shear transfer along FRP-concrete interface in flexural members, *Journal of Material, Concrete Structures and Pavements, JSCE*, Vol.49, No.662, pp.231-245.

Wu, Z.S. & Yin, J. Numerical analysis on interfacial fracture mechanism of external FRP strengthened concrete members, *Journal of Material, Concrete Structures and Pavements, JSCE* (in submittal).

Wu, Z.S., Yuan, H. & Niu, H. Stress transfer and fracture propagation in different kinds of adhesive joints, *Journal of Engineering Mechanics, ASCE* (in submittal).

Yin, J. & Wu, Z.S. 1999. Interface crack propagation in FRP-strengthened concrete structures using nonlinear fracture mechanics, FRPRCS-4, pp.1035-1047, Baltimore.

Yin, J., Wu, Z.S. & Asakura, T. FE analysis on cohesive debonding cracking behavior of FRP-strengthened concrete beams by nonlinear fracture mechanics, *ACI 2000 Spring Convention Special Publication*, CA. (in press).

Yoshizawa, H., Wu, Z.S., Yuan, H. & Toshiyuki, K. 2000. Study on FRP-concrete interface bond performance, *Jour-*

nal of Structural Mechanics And Earthquake Engineering, JSCE, Vol.49, No.662, pp.105-119. (in Japanese).
Yuan, H., Wu, Z.S. & Yoshizawa, H. Therotical solution on interfacial stress transfer of externally bonded steel/composite laminates, *Journal of Structural Mechanics And Earthquake Engineering, JSCE* (in press).